THE JOURNAL OF PHYSICAL CHEMISTRY Letters

Letter

pubs.acs.org/JPCL

Ultrafast Studies of Exciton Migration and Polaron Formation in Sequentially Solution-Processed Conjugated Polymer/Fullerene Quasi-Bilayer Photovoltaics

Alexander L. Ayzner,[†] Stephanie C. Doan, Bertrand Tremolet de Villers,[‡] and Benjamin J. Schwartz*

Department of Chemistry and Biochemistry, UCLA, Los Angeles, California 90095-1569, United States

Supporting Information

ABSTRACT: We examine the ultrafast dynamics of exciton migration and polaron production in sequentially processed 'quasi-bilayer' and preblended 'bulk heterojunction' (BHJ) solar cells based on conjugated polymer films that contain the same total amount of fullerene. We find that even though the polaron yields are similar, the dynamics of polaron production are significantly slower in quasi-bilayers than BHJs. We argue that the different polaron production dynamics result from the fact that (1) there is significantly less fullerene inside the polymer in quasi-bilayers than in BHJs and (2) sequential processing yields polymer layers that are significantly more ordered than BHJs. We also argue that thermal annealing improves the performance of quasi-bilayer solar cells not because annealing drives additional fullerene into the polymer but because annealing improves the fullerene crystallinity. All of the results suggest that sequential processing remains a viable alternative for producing polymer/fullerene solar cells with a nanometer-scale architecture that differs from BHJs.

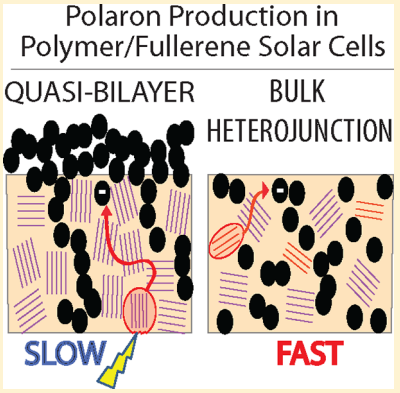

SECTION: Energy Conversion and Storage; Energy and Charge Transport

Organic solar cells based on semiconducting conjugated polymers as photoexcited electron donors and fullerene derivatives as electron acceptors have reached power conversion efficiencies in excess of 8%.[1] The conjugated polymer typically functions as the light absorber, converting incident photons to bound excitations (excitons). Excited states originating on different chain segments can migrate from one chromophore to another by means of electronic energy transfer. The distance such excitations can move during their lifetime, known as the exciton diffusion length (EDL), has been estimated in many different polymeric semiconductors to lie in the 5−10 nm range,[2−5] although higher estimates recently have been reported.[6] The idea that excitations in semiconducting polymer films cannot move very far has given rise to devices based on the bulk heterojunction (BHJ) architecture. In a BHJ device, the donor and acceptor molecules are intimately blended on a length scale roughly equal to or finer than the EDL; this ensures that the majority of excitons are able to migrate to an acceptor, where they can undergo charge separation and ultimately produce electrical current.

Although the BHJ architecture helps to ensure effective charge separation, simply blending polymers and fullerenes together frequently results in a strongly energetically and topologically disordered polymer phase with fullerene molecules nearly uniformly distributed throughout the film, a morphology that is not conducive to efficient carrier transport. Thus, most BHJ devices require additional processing, such as the use of solvent additives[7−9] or thermal[10−20] or solvent annealing,[21] which can help to crystallize the polymer or fullerene to produce a more optimal morphology for solar cell performance. Unfortunately, finding the best weight ratio of the donor and acceptor and optimizing the processing conditions for a particular set of materials is a painstaking process that largely depends on trial-and-error.

Recently, we developed a method to prepare devices by sequentially solution-depositing layers of polymer and fullerene from orthogonal solvents.[22] This allowed us to preoptimize the polymer underlayer by building in crystalline, percolated pathways for charge and exciton transport. The subsequent deposition of the fullerene overlayer had little effect on the crystallinity of the polymer underlayer, providing control over the device morphology. We prepared devices this way using the model semiconducting polymer regioregular poly(3-hexylthiophene-2,5-diyl) (P3HT), cast from *o*-dicholorobenzene (ODCB), and the well-studied fullerene derivative [6,6]-phenyl-C_{61}-butyric-acid-methyl-ester (PCBM) (see Figure 1 for chemical structures), cast from dichloromethane (DCM), and achieved power conversion efficiencies that exceeded benchmark blend-cast BHJ devices based on the same materials.[22]

In our initial report, we mistakenly believed that casting the two materials sequentially from orthogonal solvents left distinct P3HT and PCBM layers with a relatively clean interface between them.[22] Subsequently, work from several groups,[23−26]

Received: June 12, 2012
Accepted: August 1, 2012

   dx.doi.org/10.1021/jz300762c | *J. Phys. Chem. Lett.* 2012, 3, 2281−2287

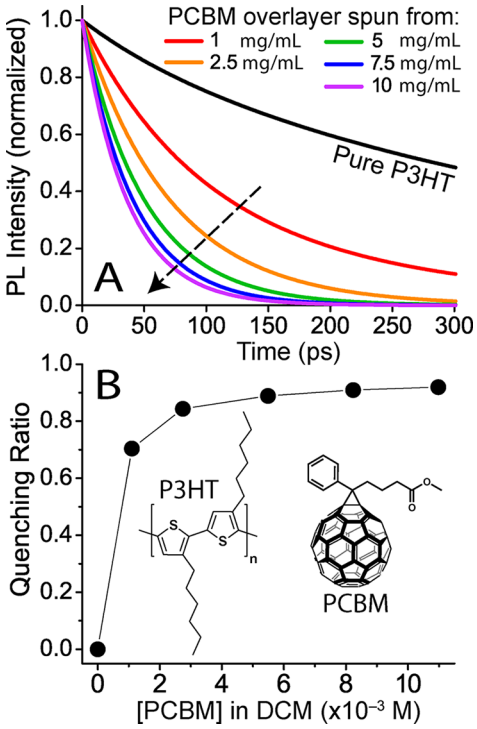

Figure 1. (A) Time-resolved photoluminescence (PL) decays for P3HT/PCBM quasi-bilayer samples with the PCBM overlayer spun from DCM solutions with different concentrations (colored curves); for reference, the PL decay of a pure P3HT film is shown as the black curve. (B) PL quenching ratio, η, defined in the main text, for the same quasi-bilayer samples whose PL dynamics are shown in panel A.

including our own,[27] revealed that some interpenetration of the fullerene into the polymer underlayer takes place in these sequentially processed films. In as-cast films, a significant fraction of the fullerene remains in a well-defined overlayer, whereas the remaining fraction disperses into the polymer underlayer with a concentration profile that is essentially uniform with depth.[25] The amount of fullerene that interpenetrates into the polymer underlayer is significantly less than that used to construct a typical BHJ.[27] Based on this knowledge, we now refer to our sequentially processed samples as 'quasi-bilayers'. A key question concerning quasi-bilayer samples is the internal distribution of fullerene molecules in the film and how this distribution compares to the active layer of a BHJ. Moon et al. have argued that sequential processing and single-layer processing as a BHJ produce the same underlying nm-scale distribution of fullerenes within the polymer layer.[28] However, Gevaerts et al. recently showed that thermal annealing affects quasi-bilayer and BHJ solar cells differently, strongly suggesting that the internal fullerene distribution is indeed different.[29]

In this Letter, we report new measurements of the ultrafast exciton quenching and polaron formation dynamics in P3HT:PCBM quasi-bilayer and BHJ thin films that contain equal total amounts of fullerene. We find that the even though the polaron yields in the two samples are similar, the exciton quenching and polaron production dynamics are quite different. This provides a strong indication that the internal fullerene distribution is indeed different between the two architectures. Our observation that the dynamics of polaron production in quasi-bilayers is slower than that in BHJs demonstrates that near-immediate exciton splitting is not necessary for efficient polaron generation. Finally, we argue that it is the crystallization of the fullerene phase and the concomitant increase in the electron mobility − *not* an increase in the donor/acceptor interfacial area − that is primarily responsible for the improvement in the power conversion efficiency of quasi-bilayers upon thermal annealing.

In our previous work, we showed that the photoluminescence (PL) of P3HT is strongly quenched by PCBM in quasi-bilayer films.[22] To better understand how this PL quenching depends on the way the fullerenes interdiffuse into the polymer layer, we have used time-resolved PL to measure the dynamics of exciton quenching in relatively thick (∼330 nm) P3HT films with fullerene overlayers cast from DCM solutions with varying PCBM concentration. Unlike steady-state PL experiments, the TCSPC technique has the advantage that the measured observable − the time decay of the PL − is negligibly affected by thin film interference. Figure 1A shows the time-resolved PL decays, deconvoluted from the instrument response function and normalized at time zero as described in the SI, for a pure P3HT film (black curve) as well as quasi-bilayers (various colored curves) prepared with different PCBM solution concentrations. Clearly, spin-coating a relatively dilute 1 mg/mL PCBM solution from DCM onto P3HT results in dramatic quenching of the polymer PL, even for underlayer thicknesses greater than 300 nm.

To quantify this quenching, we define the experimental quenching ratio

$$\eta = 1 - \int_0^\infty I_{qb}(t)\,dt \Big/ \int_0^\infty I_{P3HT}(t)\,dt$$

where I_{qb} is the (normalized) PL intensity of the quasi-bilayer film and I_{P3HT} is the PL intensity of a P3HT control film with no PCBM spun on top. Figure 1B plots the quenching ratio as a function of the concentration of the solution used to cast the PCBM overlayer. At low concentrations, the quenching ratio increases sharply with PCBM solution concentration., but as the PCBM concentration increases, η increases much more slowly, indicating that additional PCBM does not provide any significant additional quenching.

The way in which the quenching ratio changes with the concentration of the solution used to cast the PCBM overlayer has important implications for the quenching mechanism. We know from our previous work[22] (and see also the Supporting Information (SI)) that the act of fullerene layer deposition negligibly perturbs the crystallinity of the underlying P3HT layer in the quasi-bilayer architecture. However, the fact that DCM does not dissolve high-molecular-weight, regioregular P3HT does not preclude DCM from swelling the lower molecular weight or disordered P3HT in the amorphous regions of the film. Thus, casting the PCBM overlayer from DCM allows fullerenes to penetrate the amorphous regions of the P3HT underlayer without disrupting any of the P3HT crystallinity. The driving force for this interpenetration is the chemical potential gradient between the swollen polymer matrix and the fullerene solution. Increasing the fullerene solution concentration thus has two important consequences for quasi-bilayer formation: (1) the PCBM concentration gradient increases, driving more fullerene molecules into the polymer underlayer, and (2) a progressively thicker, nearly pure fullerene layer is deposited on top of the now-intermixed layer. The quenching data in Figure 1 support this idea. At low concentration, fullerenes occupy the amorphous regions of the P3HT underlayer, providing interfacial area for quenching

dx.doi.org/10.1021/jz300762c | J. Phys. Chem. Lett. 2012, 3, 2281−2287

P3HT excitons. Increasing the concentration of the PCBM casting solution drives additional fullerene into these regions but does not proportionally increase the amount of interfacial contact between P3HT and PCBM.

We next used ultrafast transient absorption spectroscopy to examine the charge generation that occurs in both quasi-bilayers and blend-cast BHJs when a P3HT exciton encounters a PCBM molecule. Figure 2 shows excited-state absorption

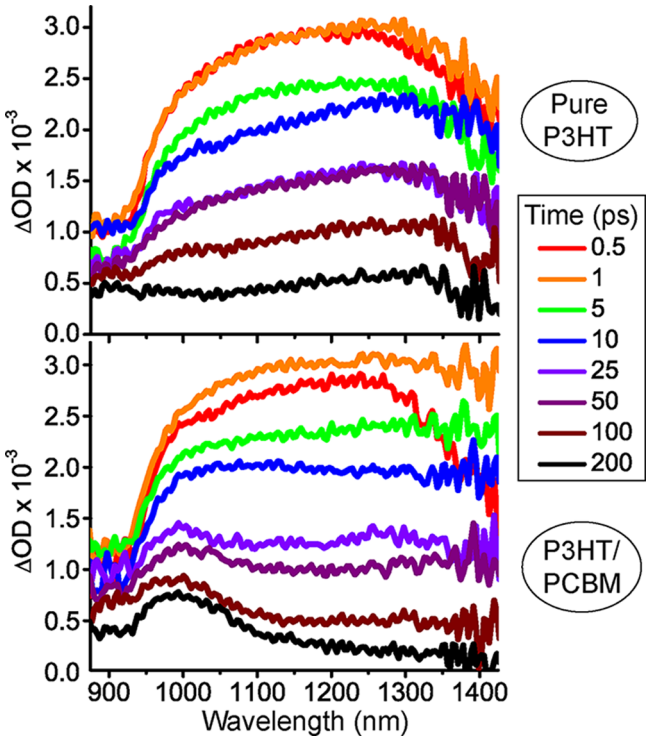

Figure 2. Ultrafast transient absorption of a pure P3HT film (upper panel) and a quasi-bilayer with a PCBM overlayer spun from a 1 mg/mL DCM solution (lower panel) following excitation at 530 nm as a function of time. The noise red of 1350 nm results from a lack of photons in the white-light continuum probe pulse at these wavelengths.

spectra at different times following excitation of P3HT in both a pristine P3HT film (upper panel) and a quasi-bilayer sample prepared with the same P3HT underlayer and an overlayer cast from a 1 mg/mL PCBM/DCM solution (lower panel). The large feature that peaks near 1150 nm has been assigned by others to be the absorption of the P3HT exciton;[30,31] this feature decays with time in both samples. In the pure P3HT sample, the exciton absorption decays to near baseline on a ~200-ps time scale. In the quasi-bilayer sample, however, the excitons decay much more quickly, and a new peak centered at 980 nm is evident at long times, which is absent in pure P3HT; this new feature has been previously assigned to absorption from P3HT hole polarons.[32−34] The data make it clear that the majority of excitons are quenched in the quasi-bilayer sample, consistent with Figure 1, and that a product of the quenching is a P3HT polaron.

To better characterize the exciton and polaron dynamics in our samples, we have decomposed the spectra from our ultrafast experiments into their constituent exciton and polaron contributions. We assumed that the spectrum at short times (<0.5 ps) was that of the pure P3HT exciton and that at long times (>200 ps) all the excitons had decayed, leaving only the spectrum of the longer-lived P3HT polarons. We then fit our measured transient absorption spectra at each time to a linear combination of the exciton and polaron spectra, as described in the SI. This analysis allowed us to compare relative polaron yields from a ratio of the spectral integral at long time, which contains only the polaron contribution, to the spectral integral of the exciton-only peak at short time.

As a way to describe these data and aid physical interpretation, with no physical model implied, we fit the exciton decay dynamics with a triple-exponential and the appearance of the polarons using a biexponential rise. The fitting parameters for the exciton and polaron dynamics are given in Table 1 and the polaron rises (symbols) and their

Table 1. Exciton and Polaron Dynamics of Different P3HT-PCBM Samples Extracted from Ultrafast Transient Absorption Spectroscopy (cf. Figure 3 and SI)[a]

film	a_1	a_2	a_3	τ_1 (ps)	τ_2 (ps)	τ_3 (ps)
Excitons:						
P3HT (200 nm)	0.22	0.36	0.31	4.5	66.2	478.5
Q-B 1 mg/mL[b]	0.24	0.32	0.51	0.4	7.6	77.8
Q-B 5 mg/mL	0.28	0.50	0.22	1.5	20.9	89.3
Q-B 12.5 mg/mL	0.27	0.49	0.24	1.1	10.8	65.5
Q-B 12.5 mg/mL AN[+]	0.21	0.42	0.40	1.1	9.2	43.4
BHJ 1:0.05	0.23	0.40	0.39	1.6	15.0	85.9
BHJ 1:0.2	0.27	0.48	0.30	0.9	13.2	72.6
BHJ 1:0.6	0.26	0.47	0.35	0.7	7.8	37.3
Polarons:						
Q-B 1 mg/mL	0.30	0.70		3.7	47.3	
Q-B 5 mg/mL	0.49	0.51		8.5	27.0	
Q-B 12.5 mg/mL	0.40	0.60		1.8	20.2	
Q-B 12.5 mg/mL AN[c]	0.47	0.53		2.0	17.8	
BHJ 1:0.05	0.37	0.63		5.1	54.3	
BHJ 1:0.2	0.54	0.46		8.8	26.3	
BHJ 1:0.6	0.41	0.59		1.8	11.5	

[a]Exciton decay dynamics were fit to the form $\sum_{i=1}^{3} a_i e^{-t/\tau_i}$, and polaron formation dynamics to $\sum_{i=1}^{2} a_i (1 - e^{-t/\tau_i})$. [b]Q-B stands for quasi-bilayer. [c]AN stands for annealed at 150 °C for 20 min. Quasi-bilayers are distinguished by the concentration of PCBM in the DCM solution used to cast the overlayer.

exponential fits (thin solid and dashed curves) are shown in Figure 3. The fast exciton quenching and polaron formation time scale, which is present in comparable proportion in all films, corresponds to exciton harvesting in the immediate vicinity of the nascent excited chromophore. Intermediate exciton decay rates likely correspond to resonant electronic energy transfer through one or several polymer aggregates in relative proximity to a heterojunction, wherein multiple transfer steps are required to find a dissociating interface. We assign the long decay time to largely incoherent energy transfer of a Förster type between transition dipoles with a finite spatial electron density extent (i.e., generalized energy transfer between nonpoint dipoles).[35] Thus, we believe that at long times (tens of picoseconds) excitations reach the donor/acceptor interface in a random walk fashion after sampling a significant number of spatially distinct, low-energy exciton "traps" over a number of polymer aggregates.

Figure 3 compares the polaron production dynamics of blend-cast BHJs (red symbols) and quasi-bilayer films (black symbols) at two different PCBM loadings. It is clear that in the

dx.doi.org/10.1021/jz300762c | J. Phys. Chem. Lett. 2012, 3, 2281−2287

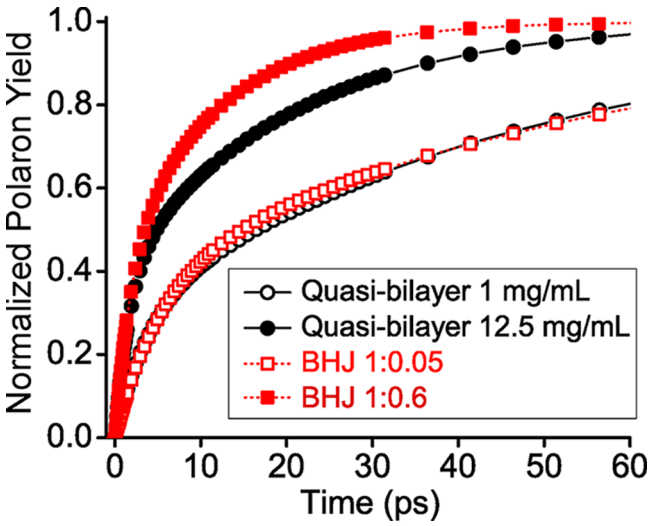

Figure 3. Dynamics of the polarons produced following 530 nm excitation of P3HT/PCBM quasi-bilayer samples with PCBM overlayers spun from DCM solutions of different concentration (black circles) and from P3HT:PCBM BHJ films with the same total amount of fullerene, as determined by UV−visible absorption (red squares). The polaron dynamics were extracted from the ultrafast transient absorption spectrum (cf. Figure 2) using the procedure outlined in the SI.

1:0.6 BHJ film (closed red squares), a significant fraction (~40%) of polarons are formed in the first few picoseconds following excitation, a result consistent with previous work that has noted that electron transfer from excited P3HT to PCBM takes place on ultrafast time scales.[36] In addition, the data also show that the remaining polarons are formed on a longer time scale (~11 ps) because some excitons must make multiple hops between P3HT chains before they can reach a PCBM molecule to produce polarons via charge transfer; this observation is consistent with recent reports.[37] What is striking about this data is that Figure 3 and Table 1 show that the long component of the exciton quenching and polaron rise in the quasi-bilayer film (12.5 mg/mL PCBM, black filled circles), which has the same total amount of fullerene as the 1:0.6 BHJ film as measured by UV−visible spectroscopy (see SI), is significantly slower (~20 ps) than that in the BHJ (~11 ps). This is particularly surprising because the polaron yield in quasi-bilayer films is similar to that in the corresponding concentration-matched blend-BHJs. It is not until we get to samples that are quite dilute in PCBM that we start to see similar slower polaron appearance time scales in BHJs as in the corresponding quasi-bilayer samples (Figure 3, open squares).

Even though our BHJ and quasi-bilayer samples were prepared to have the same total amount of PCBM, we know that in quasi-bilayers a significant fraction of the PCBM stays in the overlayer, whereas only a smaller fraction penetrates into the P3HT underlayer. Using the analysis outlined in the SI, we estimate that the fullerene density inside the P3HT underlayers in our quasi-bilayer samples is significantly lower than in the corresponding BHJ samples that have the same total amount of fullerene.[38] This makes the results in Figure 3 and Table 1 all the more intriguing and emphasizes that the PCBM that does penetrate into the quasi-bilayer does *not* lead to a film microstructure that is identical to a blend-cast BHJ.

This leads to the question of precisely what is different about exciton harvesting and charge generation in quasi-bilayers (and very dilute BHJs) than in the concentrated BHJs typically used in devices. The first obvious answer is the difference in the effective fullerene density inside of the film. The majority of excitons in concentrated BHJs are created within an EDL of an acceptor. In contrast, in quasi-bilayers, the fraction of excitons that need to make multiple hops prior to reaching a heterojunction is expected to be significantly greater than in device-optimal BHJs, so that it takes longer to quench them and produce P3HT polarons.

However, in addition to internal fullerene content, there is a second significant difference between these two solar cell architectures: the ordering of the P3HT. Indeed, the UV−visible absorption spectra shown in the SI indicate that in dilute BHJs and quasi-bilayer films, the P3HT is significantly more ordered than in BHJs loaded with PCBM at near device-optimal concentrations. We believe that the presence of considerably enhanced long-range order in P3HT films, whose interchain π-stacking interactions are unperturbed by the presence of a large number of interdiffused fullerene molecules, may increase the interchromophore and/or interaggregate excitation transfer rates and thus modify the EDL. We will demonstrate in future work that the effective EDL is greater in ordered P3HT subphases than in the largely disordered polymer phases produced in as-cast BHJs, consistent with previous work with small molecules.[39,40]

In addition to noting the differences in exciton quenching and polaron formation between quasi-bilayers and BHJs, we also have explored the behavior of quasi-bilayer ultrafast dynamics upon thermal annealing. In our previous work, we found that thermal annealing of quasi-bilayer solar cells increased both the device short-circuit current and the fill factor. However, we also saw that after annealing the total PL intensity from the polymer *increased*.[22] This suggests that annealing actually *decreases* the interfacial donor/acceptor interfacial area available for exciton dissociation. This observation seems counterintuitive because multiple studies have shown that thermal annealing increases the amount of PCBM that penetrates into the P3HT underlayer in quasi-bilayers.[24−26] To better understand why thermal annealing leads to less exciton harvesting but still improves the performance of quasi-bilayer devices, in Figure 4 we compare the exciton quenching (inset) and polaron formation dynamics (main figure) of as-cast (black symbols/curves) and annealed (blue symbols/curves) P3HT/PCBM quasi-bilayer films. The inset makes it clear that the exciton lifetime is longer, and the main figure shows that the long-time yield of polarons is smaller in annealed quasi-bilayer films than in as-cast films, consistent with the increase in steady-state PL intensity.[22] We believe that the decrease in donor/acceptor interfacial area is primarily due to fullerene aggregation and crystallization upon annealing, although we expect that a slight increase in P3HT crystallite size might also contribute.[22]

Moreover, even though the relative polaron yield is lower in annealed quasi-bilayers, on average, the appearance of polarons in annealed films occurs on a slightly faster time scale than in as-cast films. Because the interfacial area decreases upon annealing, this suggests that the conversion of excitons to polarons becomes more efficient when PCBM is crystalline, even though the yield is limited by the available surface area of the aggregated PCBM network. Thus, despite the fact that annealing drives more PCBM into the P3HT underlayer, the additional PCBM is located only in the previously PCBM-rich

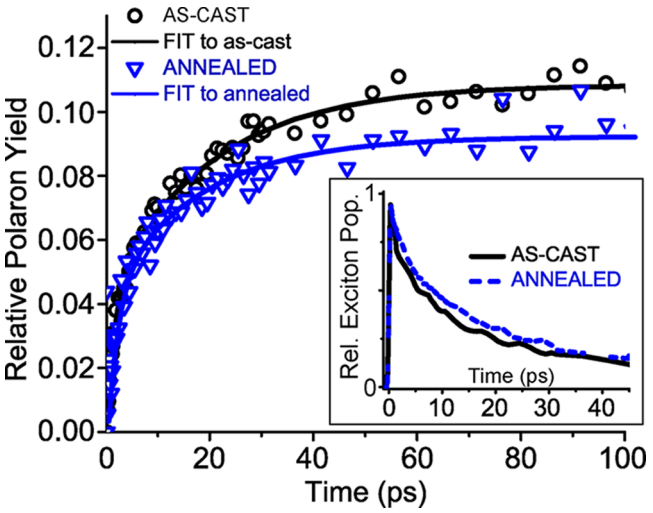

Figure 4. Polaron production (main figure) and exciton decay (inset) dynamics extracted from ultrafast transient absorption spectra (cf. Figure 2) for an as-cast P3HT/PCBM quasi-bilayer (black circles and solid curves) and the same sample after thermal annealing at 150 °C for 20 min (blue triangles and dashed curve). The samples were prepared using a PCBM overlayer spun from a 12.5 mg/mL DCM solution and the excitation wavelength was 530 nm.

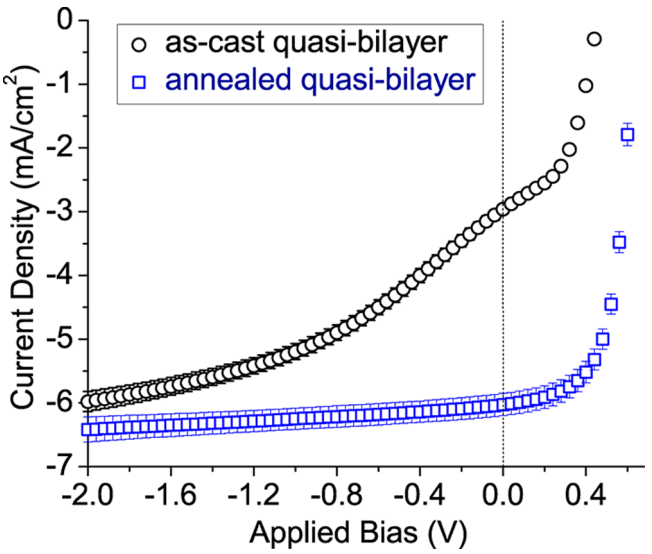

Figure 5. Current−voltage characteristics of sandwich-structure (ITO/PEDOT-PSS/quasi-bilayer/cathode) photovoltaic devices under AM 1.5 simulated solar irradiation with the active layer as-cast (black circles) or thermally annealed at 150 °C for 20 min (blue squares). The active layer was prepared using a PCBM overlayer spun from a 12.5 mg/mL DCM solution. Even though the short-circuit and reverse-bias saturation currents greatly increase upon thermal annealing, as discussed in ref 22, the PL quantum yield of the active quasi-bilayer decreases upon thermal annealing, indicating that the annealing-induced current increase does not result from increased donor/acceptor interfacial area.

amorphous regions of the film; annealing makes quasi-bilayer films less homogeneous.

In addition to thermal annealing decreasing the film homogeneity of quasi-bilayers, it also changes the local way in which the fullerenes are distributed. In our previous work, we found that thermal annealing of quasi-bilayers led to crystallization of the fullerene network, whereas the morphology of the polymer underwent only minor changes.[22] Hence, we expect that thermal annealing negligibly improves the hole mobility,[41] and the increased PL/lower polaron yield demonstrates that thermal annealing actually leads to poorer exciton harvesting. This means that the annealing must increase the electron mobility by a significant factor to give the observed improvement in solar cell performance.

Additional evidence of improvement in the electron mobility upon thermal annealing of quasi-bilayers can be found in the reverse bias region of the device photocurrent, shown in Figure 5. The current of the as-cast film exhibits an inflection point and does not approach saturation until large reverse bias. In contrast, the current of the thermally annealed device has the desired diodic shape and reaches saturation much earlier than its as-cast analogue. We believe that the reason for the inflection point in the as-cast curve is as follows. When the quasi-bilayer film is cast from a high vapor pressure solvent, the fullerene network exhibits low crystallinity and thus low electron mobility. Upon application of increasing reverse bias, the electric field in the as-cast device becomes sufficiently strong to overcome the fact that interfullerene jumps are inefficient at low field. Only at high fields do the electron hops become rapid enough that the effective hole and electron mobilities become comparable, allowing the as-cast cell to approach the saturation current of the annealed device. Thus, we believe that the improvement in device performance upon thermal annealing of quasi-bilayers primarily results from the increased aggregation and partial crystallization of the fullerene network, *not* from the additional fullerene that migrates into the polymer underlayer.

In summary, we have found that the dynamics of exciton quenching and polaron formation in P3HT/PCBM films are different if the P3HT and PCBM are deposited from a single solution or deposited sequentially from separate solutions using orthogonal solvents: sequential processing is *not* simply another route to producing a blended BHJ. This is because when P3HT and PCBM are deposited sequentially, the P3HT has a higher degree of interchain ordering than when the two materials are deposited together in a BHJ. The PCBM in as-cast quasi-bilayers is localized in the amorphous regions of the P3HT underlayer, and some fraction of the PCBM remains on top, so that there is significantly less PCBM inside the P3HT underlayer in quasi-bilayer samples than in BHJ samples with the same P3HT:PCBM ratio. Quasi-bilayers with increased P3HT crystallinity display quite different time scales for polaron production than the concentrated BHJs typically used in working photovoltaic devices, even though the total polaron yield remains similar. All of these results support the conclusions that the internal fullerene distribution in quasi-bilayers is different from that in blend-cast BHJs and that slower exciton-to-polaron conversion need not be detrimental to device performance. This partially relaxes the requirement for high area of the donor/acceptor interface. Finally, we also argued that thermal annealing improves the performance of quasi-bilayers not because increased fullerene concentration in the underlayer makes them more like BHJs but because of an increase in fullerene crystallinity that improves the electron mobility. Together, all of this work suggests that sequential processing is a real and viable alternative to BHJ for the production of conjugated polymer/fullerene photovoltaic devices.

dx.doi.org/10.1021/jz300762c | *J. Phys. Chem. Lett.* 2012, 3, 2281−2287

■ ASSOCIATED CONTENT

Supporting Information

Steady-state PL and UV−vis spectroscopy, experimental details, spectral fitting procedures and discussion of potential errors, and TCSPC deconvolution description. This material is available free of charge via the Internet at http://pubs.acs.org

■ AUTHOR INFORMATION

Corresponding Author

*E-mail: schwartz@chem.ucla.edu.

Present Addresses

[†]Stanford Synchrotron Radiation Lightsource, SLAC National Accelerator Laboratory, Menlo Park, CA 94025.

[‡]Materials Department, University of California, Santa Barbara, CA 93106-5050.

Notes

The authors declare no competing financial interest.

■ ACKNOWLEDGMENTS

This work was supported as part of an Energy Frontiers Research Center, "Molecularly Engineered Energy Materials (MEEM)", funded by the U.S. Dept. of Energy, Office of Science, Office of Basic Energy Sciences under contract no. DE-SC0001342:001. Partial support for ALA and BTdV also was provided by the National Science Foundation (NSF) under grant number CHE-1112569, and partial support for SCD was provided under NSF grant CHE-0908548. Support for one of the laser systems used in this work was provided by NSF grant CHE-0741804. We are grateful for Alexander Mikhailovsky's (UCSB) help with the TCSPC measurements, and we also thank Thomas Quickel (Intel Corp.) for help with profilometry measurements.

■ REFERENCES

(1) Green, M. A.; Emery, K.; Hishikawa, Y.; Warta, W.; Dunlop, E. D. Solar Cell Efficiency Tables (v. 39). *Prog. Photovoltaics Res. Appl.* **2012**, *20*, 12−20.

(2) Lewis, a. J.; Ruseckas, a.; Gaudin, O. P. M.; Webster, G. R.; Burn, P. L.; Samuel, I. D. W. Singlet Exciton Diffusion in MEH-PPV Films Studied by Exciton-Exciton Annihilation. *Org. Electron.* **2006**, *7*, 452−456.

(3) Mikhnenko, O. V.; Cordella, F.; Sieval, A. B.; Hummelen, J. C.; Blom, P. W. M.; Loi, M. A. Temperature Dependence of Exciton Diffusion in Conjugated Polymers. *J. Phys. Chem. B* **2008**, *112*, 11601−11604.

(4) Markov, D. E.; Amsterdam, E.; Blom, P. W. M.; Sieval, A. B.; Hummelen, J. C. Accurate Measurement of the Exciton Diffusion Length in a Conjugated Polymer Using a Heterostructure with a Side-Chain Cross-Linked Fullerene Layer. *J. Phys. Chem. A* **2005**, *109*, 5266−5274.

(5) Shaw, P. E.; Ruseckas, A.; Samuel, I. D. W. Exciton Diffusion Measurements in Poly(3-hexylthiophene). *Adv. Mater.* **2008**, *20*, 3516−3520.

(6) Cook, S.; Liyuan, H.; Furube, A.; Katoh, R. Singlet Annihilation in Films of Regioregular Poly(3-hexylthiophene): Estimates for Singlet Diffusion Lengths and the Correlation between Singlet Annihilation Rates and Spectral Relaxation. *J. Phys. Chem. C* **2010**, *114*, 10962−10968.

(7) Liu, X.; Huettner, S.; Rong, Z.; Sommer, M.; Friend, R. H. Solvent Additive Control of Morphology and Crystallization in Semiconducting Polymer Blends. *Adv. Mater.* **2012**, *24*, 669−674.

(8) Koetniyom, W.; Keawprajak, A.; Piyakulawat, P.; Jiramitmongkon, K.; Nukeaw, J.; Pratontep, S.; Asawapirom, U. Effect of Trichlorobenzene Additive on the Performance and Morphology of Polyfluorene and Fullerene Derivative Bulk Heterojunction Solar Cells. *Can. J. Chem. Eng.* **2012**, *90*, 897−902.

(9) Rogers, J. T.; Schmidt, K.; Toney, M. F.; Kramer, E. J.; Bazan, G. C. Structural Order in Bulk Heterojunction Films Prepared with Solvent Additives. *Adv. Mater.* **2011**, *23*, 2284−2288.

(10) Huang, Y.-C.; Chuang, S.-Y.; Wu, M.-C.; Chen, H.-L.; Chen, C.-W.; Su, W.-F. Quantitative Nanoscale Monitoring the Effect of Annealing Process on the Morphology and Optical Properties of Poly(3-hexylthiophene)/[6,6]-Phenyl C_{61}-Butyric Acid Methyl Ester Thin Film Used in Photovoltaic Devices. *J. Appl. Phys.* **2009**, *106*, 034506-1−034506-6.

(11) McNeill, C. R.; Halls, J. J. M.; Wilson, R.; Whiting, G. L.; Berkebile, S.; Ramsey, M. G.; Friend, R. H.; Greenham, N. C. Efficient Polythiophene/Polyfluorene Copolymer Bulk Heterojunction Photovoltaic Devices: Device Physics and Annealing Effects. *Adv. Funct. Mater.* **2008**, *18*, 2309−2321.

(12) Marsh, R. A.; Hodgkiss, J. M.; Albert-Seifried, S.; Friend, R. H. Effect of Annealing on P3HT:PCBM Charge Transfer and Nanoscale Morphology Probed by Ultrafast Spectroscopy. *Nano Lett.* **2010**, *10*, 923−930.

(13) Cho, S.; Lee, K.; Yuen, J.; Wang, G.; Moses, D.; Heeger, A. J.; Surin, M.; Lazzaroni, R. J. Thermal Annealing-Induced Enhancement of the Field-Effect Mobility of Regioregular Poly(3-hexylthiophene) Films. *J. Appl. Phys.* **2006**, *100*, 114503.

(14) Hiorns, R. C.; de Bettignies, R.; Leroy, J.; Bailly, S.; Firon, M.; Sentein, C.; Khoukh, a.; Preud'homme, H.; Dagron-Lartigau, C. High Molecular Weights, Polydispersities, and Annealing Temperatures in the Optimization of Bulk-Heterojunction Photovoltaic Cells Based on Poly(3-hexylthiophene) or Poly(3-butylthiophene). *Adv. Funct. Mater.* **2006**, *16*, 2263−2273.

(15) Gao, Y.; Grey, J. K. Resonance Chemical Imaging of Polythiophene/Fullerene Photovoltaic Thin Films: Mapping Morphology-Dependent Aggregated and Unaggregated C═C Species. *J. Am. Chem. Soc.* **2009**, *131*, 9654−9662.

(16) Yang, F.; Shtein, M.; Forrest, S. R. Controlled Growth of a Molecular Bulk Heterojunction Photovoltaic Cell. *Nat. Mater.* **2005**, *4*, 37−41.

(17) Swinnen, A.; Haeldermans, I.; vande Ven, M.; D'Haen, J.; Vanhoyland, G.; Aresu, S.; D'Olieslaeger, M.; Manca, J. Tuning the Dimensions of C60-Based Needlelike Crystals in Blended Thin Films. *Adv. Funct. Mat.* **2006**, *16*, 760−765.

(18) Kim, Y.; Cook, S.; Tuladhar, S. M.; Choulis, S. A.; Nelson, J.; Durrant, J. R.; Bradley, D. D. C.; Giles, M.; McCulloch, I.; Ha, C.-S.; Ree, M. A Strong Regioregularity Effect in Self-Organizing Conjugated Polymer Films and High-Efficiency Polythiophene:Fullerene Solar Cells. *Nat. Mater.* **2006**, *5*, 197−203.

(19) Swinnen, A.; Haeldermans, I.; Vanlaeke, P.; Haen, J. D.; Poortmans, J.; Olieslaeger, M. D.; Manca, J. V. Dual Crystallization Behaviour of Polythiophene/Fullerene Blends. *Eur. Phys. J. Appl. Phys.* **2007**, *256*, 251−256.

(20) Savenije, T. J.; Kroeze, J. E.; Yang, X.; Loos, J. The Effect of Thermal Treatment on the Morphology and Charge Carrier Dynamics in a Polythiophene−Fullerene Bulk Heterojunction. *Adv. Funct. Mater.* **2005**, *15*, 1260−1266.

(21) Kumar, A.; Li, G.; Hong, Z.; Yang, Y. High Efficiency Polymer Solar Cells with Vertically Modulated Nanoscale Morphology. *Nanotechnology* **2009**, *20*, 165202.

(22) Ayzner, A. L.; Tassone, C. J.; Tolbert, S. H.; Schwartz, B. J. Reappraising the Need for Bulk Heterojunctions in Polymer-Fullerene Photovoltaics: The Role of Carrier Transport in All-Solution-Processed P3HT/PCBM Bilayer Solar Cells. *J. Phys. Chem. C* **2009**, *113*, 20050−20060.

(23) Collins, B. A.; Tumbleston, J. R.; Ade, H. Miscibility, Crystallinity, and Phase Development in P3HT/PCBM Solar Cells: Toward an Enlightened Understanding of Device Morphology and Stability. *J. Phys. Chem. Lett.* **2011**, *2*, 3135−3145.

(24) Labram, J.; Kirkpatrick, J.; Bradley, D.; Anthopoulos, T. Measurement of the Diffusivity of Fullerenes in Polymers Using

Bilayer Organic Field Effect Transistors. *Phys. Rev. B* **2011**, *84*, 075344-1−075344-8.
(25) Lee, K. H.; Schwenn, P. E.; Smith, A. R. G.; Cavaye, H.; Shaw, P. E.; James, M.; Krueger, K. B.; Gentle, I. R.; Meredith, P.; Burn, P. L. Morphology of All-Solution-Processed "Bilayer" Organic Solar Cells. *Adv. Mater.* **2010**, *23*, 766−770.
(26) Treat, N. D.; Brady, M. a.; Smith, G.; Toney, M. F.; Kramer, E. J.; Hawker, C. J.; Chabinyc, M. L. Interdiffusion of PCBM and P3HT Reveals Miscibility in a Photovoltaically Active Blend. *Adv. Energy Mater.* **2010**, *1*, 82−89.
(27) Nardes, A. M.; Ayzner, A. L.; Hammond, S. R.; Ferguson, A. J.; Schwartz, B. J.; Kopidakis, N. Photoinduced Charge Carrier Generation and Decay in Sequentially Deposited Polymer/Fullerene Layers: Bulk Heterojunction vs Planar Interface. *J. Phys. Chem. C* **2012**, *116*, 7293−7305.
(28) Moon, J. S.; Takacs, C. J.; Sun, Y.; Heeger, A. J. Spontaneous Formation of Bulk Heterojunction Nanostructures: Multiple Routes to Equivalent Morphologies. *Nano Lett.* **2011**, *11*, 1036−1039.
(29) Gevaerts, V. S.; Koster, L. J. A.; Wienk, M. M.; Janssen, R. a J. Discriminating Between Bilayer and Bulk Heterojunction Polymer:-Fullerene Solar Cells using the External Quantum Efficiency. *ACS Appl. Mater. Interfaces.* **2011**, *3*, 3252−3255.
(30) Hwang, In-W.; Moses, D.; Heeger, A. J. Photoinduced Carrier Generation in P3HT/PCBM Bulk Heterojunction Materials. *J. Phys. Chem. C* **2008**, *112*, 4350−4354.
(31) Cook, S.; Furube, A.; Katoh, R. Analysis of the Excited States of Regioregular Polythiophene P3HT. *Energy Environ. Sci.* **2008**, *1*, 294−299.
(32) Guo, J.; Ohkita, H.; Benten, H.; Ito, S. Near-IR Femtosecond Transient Absorption Spectroscopy of Ultrafast Polaron and Triplet Exciton Formation in Polythiophene Films with Different Regioregularities. *J. Am. Chem. Soc.* **2009**, *131*, 16869−16880.
(33) Lioudakis, E.; Alexandrou, I.; Othonos, A. Ultrafast Dynamics of Localized and Delocalized Polaron Transitions in P3HT/PCBM Blend Materials: The Effects of PCBM Concentration. *Nanoscale Res. Lett.* **2009**, *4*, 1475−1480.
(34) Piris, J.; Dykstra, T. E.; Bakulin, A. A.; Loosdrecht, P. H. M. V.; Knulst, W.; Trinh, M. T.; Schins, J. M.; Siebbeles, L. D. A. Photogeneration and Ultrafast Dynamics of Excitons and Charges in P3HT/PCBM Blends. *J. Phys. Chem. C* **2009**, *113*, 14500−14506.
(35) Scholes, G. D.; Jordanides, X. J.; Fleming, G. R. Adapting the Förster Theory of Energy Transfer for Modeling Dynamics in Aggregated Molecular Assemblies. *J. Phys. Chem. B* **2001**, *105*, 1640−1651.
(36) Cravino, A.; Sariciftci, N. S. Conjugated Polymer/Fullerene Based Organic Solar Cells. *Proceedings of the European Meeting on High Efficiency Solar Cells* **2001**, 15−16.
(37) Zhang, W.; Hu, R.; Li, D.; Huo, M.-M.; Ai, X.-C.; Zhang, J.-P. Primary Dynamics of Exciton and Charge Photogeneration in Solvent Vapor Annealed P3HT/PCBM Films. *J. Phys. Chem. C* **2012**, *116*, 4298−4310.
(38) See the SI for details about these estimates.
(39) Gregg, B. A.; Sprague, J.; Peterson, M. W. Long-Range Singlet Energy Transfer in Perylene Bis(phenethylimide) Films. *J. Phys. Chem. B* **1997**, *101*, 5362−5369.
(40) Adams, D. M.; Kerimo, J.; O'Connor, D. B.; Barbara, P. F. Spatial Imaging of Singlet Energy Migration in Perylene bis-(phenethylimide) Thin Films. *J. Phys. Chem. A* **1999**, *103*, 10138−10143.
(41) This is consistent with a minor change in the injected current density of P3HT diodes upon annealing when the P3HT layer had been spin-coated from the slowly evaporating ODCB.